2024 IEEE International Conference on Bioinformatics and Biomedicine (BIBM) | 979-8-3503-8622-6/24/$31.00 ©2024 IEEE | DOI: 10.1109/BIBM62325.2024.10822545

UWHeart: Periodicity-Driven Contact-free Heartbeat Rate Estimation Based on IR-UWB Technology

1st Yang Cao
School of Bell Honors
Nanjing University of Posts and Telecommunications
Nanjing, China
b21060227@njupt.edu.cn

2nd Yuhao Dai
School of Computer
Nanjing University of Posts and Telecommunications
Nanjing, China
1222045629@njupt.edu.cn

3rd Dongzi Wang
School of Computer
Nanjing University of Posts and Telecommunications
Nanjing, China
2023040504@njupt.edu.cn

4th Zhengxin Guo*
School of Computer
Nanjing University of Posts and Telecommunications
Nanjing, China
guozx@njupt.edu.cn

5th Linqing Gui
School of Computer
Nanjing University of Posts and Telecommunications
Nanjing, China
guilg@njupt.edu.cn

6th Fu Xiao
School of Computer
Nanjing University of Posts and Telecommunications
Nanjing, China
xiaof@njupt.edu.cn

***Abstract*—Current RF-based solutions have demonstrated that human heartbeat activity induces millimeter-scale chest displacements, changing RF reflection paths and making contact-free heartbeat monitoring possible. However, human heartbeat activity is very weak and can be hidden by out by the body movements or breathing, which poses significant challenges in accurately extracting heartbeat information. To solve this, in this paper we propose a contact-free heartbeat rate estimation system based on the periodic variation feature, namely UWHeart. UWHeart utilizes Impulse Radio-Ultra Wideband (IR-UWB) to capture reflection signals from the monitoring target and outputs the heartbeat rate. This system first filters out the noise unrelated to heartbeat through band-pass filtering. Then, we leverage the periodicity of heartbeat activity to construct autocorrelation matrix features of the denoised signal. Finally, we develop a one-dimensional Temporal Convolutional Network (TCN) model to realize the mapping between the heartbeat autocorrelation features and actual heartbeats, and accurately estimate the heartbeat rate of the monitoring target. We also implement the UWHeart system on commercial IR-UWB equipment to verify our method through a series of experiments, and the experimental results prove the effectiveness of our method.**

***Index Terms*—Heartbeat rate monitoring, IR-UWB, autocorrelation matrix, dimensional Temporal Convolutional Network (TCN), contact-free sensing**

I. Introduction

Cardiovascular disease (CVD) has been the leading cause of mortality worldwide, with deaths rising from 12.4 million in 1990 to 19.8 million in 2022, driven by population growth, aging, and preventable risk factors [1] [2]. As a result, vital signs monitoring has gained prominence in health analysis and disease diagnosis [3] [4].

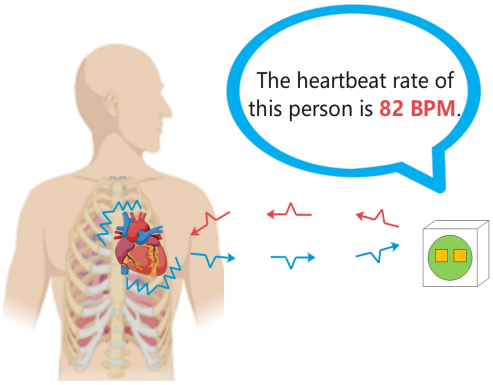

Fig. 1. The illusion of human heartbeat rate estimation.

Wearable monitoring devices, such as smart watches [5] and bracelets [6], are common, but they are inconvenient for the elderly, especially those with skin conditions, and unsuitable for continuous monitoring. Recent studies have demonstrated the potential of contact-free methods [7], [8] for high-precision human heartbeat detection by analyzing signals reflected from the body [9] [10].

Impulse Radio-Ultra Wideband (IR-UWB) technology, known for its ultra-wide bandwidth, has been shown to accurately detect human respiration and heartbeat signals [11], [12]. Recovering the heartbeat rate provides important medical insights. However, previous studies [13], [14] rely on stationary subjects close to the device, limiting their practicality. Movement after exercise introduces signal distortion, further complicating detection.

Accurately estimating the heartbeat rate faces two key challenges: filtering the weak heartbeat signal from noise,

* Corresponding author.

This work is supported in part by the National Science Fund for Distinguished Young Scholars of China under grant No.62125203, The Key Program of the National Natural Science Foundation of China under grant No.61932013 and The Key of P&D Plans of Jiangsu Provice under Grant No.BE2022798.

979-8-3503-8622-6/24/$31.00 ©2024 IEEE

and ensuring precision in post-movement states. Traditional methods fail to achieve this in dynamic scenarios due to interference from body movements and breathing.

To address these challenges, we propose UWHeart, a contact-free heartbeat rate estimation system using IR-UWB. The system preprocesses the signal, estimates chest position, generates an autocorrelation matrix, and uses a one-dimensional Temporal Convolutional Network (TCN) for heartbeat monitoring. Experiments demonstrate an average error of 4.1 bpm.

In summary, the main contributions of this paper are as follows:

- We design a contact-free heartbeat rate estimation system, which uses IR-UWB and is based on the periodicity feature of heartbeat signal.
- Our system proposes a feature mapping method of autocorrelation matrix, which is capable of constructing features based on the heartbeat signals showing periodic variations.
- We develop a one-dimensional Temporal Convolutional Network (TCN) model to establish a mapping relationship between features and the real hearbeat cycle, which automatically outputs the heartbeat rate.
- We conduct extensive experimental tests, and the results demonstrate our method can achieve accurate contact-free heartbeat rate estimation under different users, orientations, and postures.

II. System design

A. Background on IR-UWB

IR-UWB technology is a wireless carrier communication technology, which can realize high-frequency data transmission. IR-UWB demodulates the received signal $R(t)$ into a complex signal after I/Q frequency conversion at the receiver side:

$$R(t) = I(t) + jQ(t) \tag{1}$$

where I and Q are the real and imaginary part of the received signal, respectively.

In practice, the received signal amplitude $R(t)$ is represented as a 2-D Channel Impulse Response (CIR) matrix, with fast time corresponding to individual signal frames and slow time representing consecutive frames over time. The signal matrix $R(t)$ is formed by stacking these frames in time order and can be expressed as:

$$R\left(t\right) = \begin{bmatrix} r_t\left(1\right) & \cdots & r_t\left(d\right) \\ \vdots & \ddots & \vdots \\ r_1\left(1\right) & \cdots & r_1\left(d\right) \end{bmatrix} \tag{2}$$

where d is the corresponding range bin and t is the time length representing the received signal frames of each range bin. Thus the received signal matrix $R(t)$ reflects the environmental information in both time and space dimensions.

CIR can be decomposed into:

$$d\left(t\right) = \overline{d} + d^E\left(t\right) + d^B\left(t\right) + d^H\left(t\right) \tag{3}$$

where $\overline{d}$ is the average distance between the radar and the object, $d^E\left(t\right)$,$d^B\left(t\right)$ and $d^H\left(t\right)$ are the changes induced by body motion, breathing and heartbeat, respectively.

The key idea of using RF signal to detect the above distance change is to extract the amplitude and phase change of CIR $s(t)$, which the received signal becomes:

$$y\left(t\right) = \alpha\left(t\right) e^{-j2\pi f_c \frac{2d(t)}{c}} s\left(t - \frac{2d\left(t\right)}{c}\right) \tag{4}$$

where c denotes the speed of the radio wave and f_c denotes the carrier frequency.

B. System Overview

Our proposed method for contact-free heartbeat rate extraction, as shown in Figure 2, consists of four key steps: signal preprocessing, sensing area estimation, autocorrelation matrix generation, and heartbeat rate estimation. First, we align the radar data using a Butterworth filter to remove noise and isolate heartbeat-related signals. Then, we estimate the chest position by calculating Doppler shifts and respiratory energy, and generate autocorrelation matrices from the IR-UWB reflection signals, capturing long-term dependencies and periodic features. Finally, the one-dimensional Temporal Convolutional Network maps these features to accurately estimate the heartbeat rate, achieving precise, contact-free monitoring.

C. Signal Preprocessing

The collected data contains noise primarily from body movement and respiration. Respiration typically ranges between 12∼20 bpm, while body movement noise exceeds 100 Hz. The human heartbeat frequency is usually 60∼180 bpm, corresponding to 1∼3 Hz in the received signal. To isolate the relevant heartbeat signals, we apply a Butterworth bandpass filter to the radar's I and Q components, filtering out the 1∼3 Hz range. After filtering, we segment the raw signal data into 30-second samples for further analysis.

D. Heartbeat Feature Extraction

1) Sensing area estimation: Since the heart is positioned near the lungs, the reflected signal from the surrounding area can theoretically be used to extract the heartbeat waveform. However, environmental factors make this challenging. To accurately estimate the chest cavity position, we use the Respiratory Power Ratio (RPR) based on Distributed Doppler Shift (DDS). As breathing causes periodic chest displacement, which affects the IR-UWB pulse signal path, RPR helps identify the center of the chest cavity in both stationary and post-motion states.

The RPR is calculated by determining the Doppler shift at each distance point of the received signal and summing the energy within the respiratory frequency range (10–37 bpm). A comparison of the energy reflected from human activities (within -50 to 50 Hz) helps pinpoint the respiratory frequency and heartbeat location. To improve accuracy, the search area is expanded around the point of maximum RPR, covering the chest cavity, with a resolution of 0.0514 m and a range

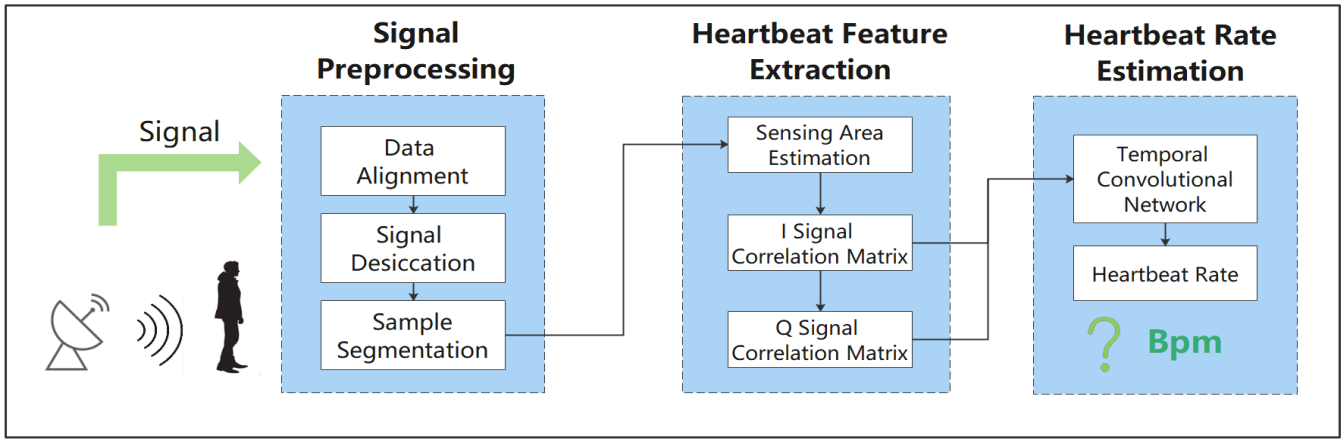

Fig. 2. The overview of UWHeart system.

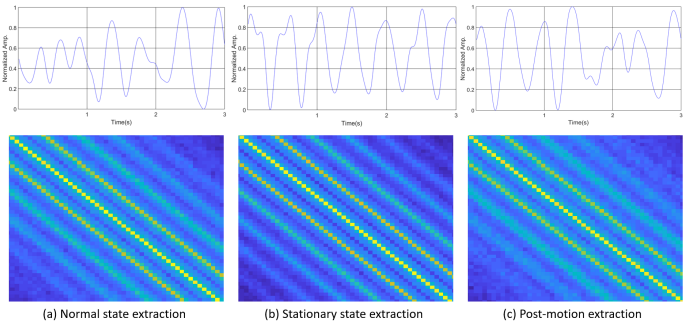

Fig. 3. The data distribution formed by the autocorrelation matrix formed by three typical heartbeat segments.

bin length of 0.3598 m, corresponding to the chest cavity's dimensions.

2) Autocorrelation matrix generation: The principle of heartbeat rate measurement by autocorrelation function is based on the periodicity of the heartbeat signal. Typically, heartbeat signals show regular fluctuations, which makes the signal autocorrelated in time, i.e., some parts of the time axis are correlated with other parts [15]. The peaks of the autocorrelation function correspond to the periodic features in the heartbeat signal, and because the signal is more similar to itself at different points in time, the autocorrelation function is higher at the correlation peaks. By measuring the time interval between these peaks, the period of the heartbeat signal can be obtained.

To extract the periodic features of the signal, we use the autocorrelation matrix as a representative feature of the heartbeat signal, capturing the periodic similarities. Autocorrelation matrices can more comprehensively capture correlations between multiple variables at different time points, which is particularly useful for data with both temporal and spatial dimensions, such as UWB data. They help in understanding spatio-temporal relationships. Vital signals have a complex structure, including multiple interwoven periodic components (e.g., breathing, heartbeat, blinking), making autocorrelation matrices ideal for analyzing this complexity [16]. Additionally, they study the periodicity of multiple variables, providing comprehensive information rather than being limited to a single variable's periodicity. Finally, autocorrelation matrices are more suitable for statistical significance tests than autocorrelation functions, enabling validation of the observed relationships.

After obtaining the reflected signals from the heartbeat region, correlation features are extracted from the I and Q signals as two-way features. Given the periodic nature of the heartbeat, the signal sequence is sliced, with the slice length correlated to the heartbeat frequency. To ensure efficient sensing, one-minute heartbeats are segmented, and an autocorrelation matrix is computed for each segment. The resulting data distribution of several typical segments is shown in Figure 3. An autocorrelation matrix describes the interdependence between random variables, where element $C(i,j)$ represents the correlation between X_i and X_j. Mathematically, the autocorrelation matrix is defined as:

$$C = C(i,j)_{n\times n} = (E[X(t)X(t+i-j)])_{n\times n} = r(i,j)_{n\times n} \quad (5)$$

where $E_{i,j}$ denotes the expectation, i and j represent the time delay indexes used to calculate the autocorrelation, $r(i,j)$ denotes the autocorrelation coefficient, $X(t)$ denotes the value of the human heartbeat signal at moment t, and $X(t+i-j)$ denotes the value of the human heartbeat signal at moment $t+i-j$.

Analyzing the autocorrelation matrices for the three cases, it can be seen that the UWHeart system can obtain autocorrelation matrices with temporal correlation in the three cases, in which the diagonal lines represent the periodic features corresponding to the segment of data. The periodicity is most obvious when the user is in a stationary state, and becomes weaker when the user is in motion due to his own shaking and the influence of respiration, which is mainly reflected in the blurring of the data at the edge of the autocorrelation matrix. However, in this scenario, the method can still obtain the periodic changes caused by the heartbeat.

E. Heartbeat rate estimation

In this paper, we propose to use the one-dimensional Temporal Convolutional Network model to complete the feature

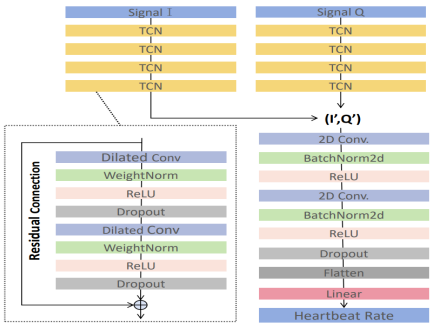

Fig. 4. The structure of the one-dimensional TCN model.

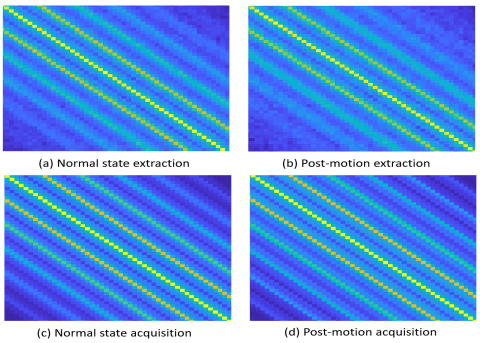

Fig. 5. The comparisons of results for TCN.

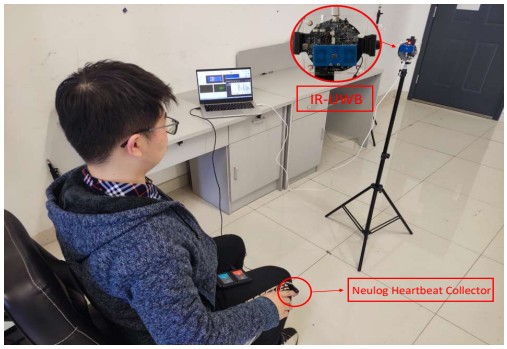

Fig. 6. The experimental scenario.

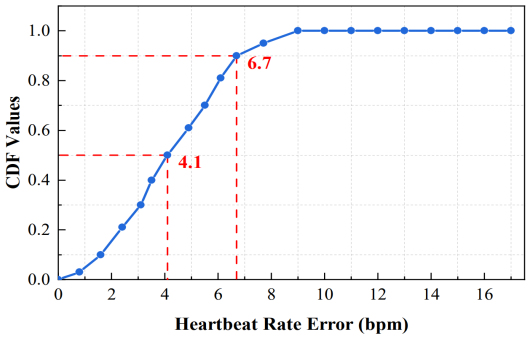

Fig. 7. The CDF values of heartbeat rate error.

mapping between the two autocorrelation matrices of the I and Q signals and the autocorrelation matrix of the heartbeat rate extracted from the real heartbeat acquisition module and combine with the convolutional autocoder to complete the monitoring of the final heartbeat rate.

The structure of the one-dimensional Temporal Convolutional Network is shown in Figure 4. The I and Q signals enter the TCN model respectively to get (I', Q'). The (I', Q') continued to be convolved and pooled twice. Then it is flattened and then passed through a linear layer to get the heartbeat rate. The TCN model consists of two dilated convolutional layers with different input channels and output channels and finally residuals are connected to avoid overfitting.

TCN outperforms other types of neural networks because they utilize a convolutional layer with an extended kernel to capture very long dependencies in the samples while maintaining a manageable number of parameters. As shown in Figure 4, the designed network model consists of an input layer, four TCN blocks, a convolutional autocoding layer module and an output layer.

The network model includes four TCN Block layers, which serve as basic building blocks. TCN is a deep learning model designed for sequential data, ideal for capturing continuous temporal dependencies. It uses temporal convolutional operations to capture long-term dependencies by applying convolutional filters along the time dimension, allowing it to detect dependencies across different time intervals. These convolution kernels perform sliding window operations on the input sequence to capture the dependencies between different time steps. Taking the first dilated convolution as an example, it takes $\{\hat{x}_n\}_{1\leq n\leq N_s}$ as input, applying dilated convolution to it with N_{ch} 1D-kernels to obtain a N_{ch}-channeled output $\{z_n\}_{1\leq n\leq N_s}$ for the next layer. For the k-th channel of the output (k= 1,...,N_{ch}), given the 1D-kernel $F_k = (f_{k,1}, ..., f_{k,L})$ with $f_{k,l}\epsilon\mathbb{R}^{N_F}(l = 1, ..., L)$ and L being the kernel size, the dilated convolution can be expressed as:

$$z_{k,n} = \Sigma_{i=0}^{L-1} f_{k,i+1}^{T} \hat{x}_{n-\chi\cdot i} \ , \ \forall n\epsilon\{1, ..., N_s\} \tag{6}$$

where $\{\hat{x}_n\}$ is zero-padded for $n < 1$, $(\cdot)^T$ is the transpose operator, and $\chi\epsilon\mathbb{Z}^+$ denotes the dilation factor used to expand the receptive field of the output element.

When training the one-dimensional TCN model, we use the Mean Squared Error(MSE) as a loss function to help the model learn how to minimize the difference between the predicted and true values. With the backpropagation algorithm, the model continuously adjusts its parameters to reduce the MSE, thus improving the accuracy of the prediction, and the loss function can be expressed as:

$$MSE = \frac{1}{N}\sum_{i=1}^{N}(y_i - \hat{y}_i)^2 \tag{7}$$

where N is the number of samples, y is the true value of the sample, and $\hat{y}$ is the predicted value of the model for the sample.

In each TCN Block layer, two inflated convolutional layers are included. By increasing the spacing in the convolutional kernel, the inflated convolution can better capture a wider

range of contextual information without increasing the number of parameters, thus extracting richer features. All four layers use weight normalization and ReLU activation functions, while a dropout layer is added to prevent overfitting with faster training convergence. The four TCN Block layers in the model are set with expansion coefficients of 1, 2, 4 and 8, respectively.

A comparison of the results of TCN is shown in Figure 5. From the figure, it can be seen that by performing feature mapping, TCN maps the coarse-grained autocorrelation matrix into a more fine-grained autocorrelation matrix, thus laying the foundation for achieving high-precision heartbeat rate estimation. Both scenarios can achieve high-precision heartbeat rate detection.

After merging the I and Q signals into one channel, we performed two 2D convolution operations to extract spatial features. To improve training speed and stability, we applied batch normalization, followed by the ReLU activation function for nonlinearity. Another 2D convolution, along with batch normalization and ReLU, was used to further refine features. The output was then flattened into a 1D vector and processed by a fully connected layer, mapping it to the final heartbeat rate.

III. Experiments and result analysis

In this section, we will evaluate the capability of the above human heartbeat rate extraction method, which we validated experimentally given several realistic scenarios and various parameter settings.

A. Experimental settings

We recruited 7 subjects (4 females and 3 males) aged 21-30 years and weighing 50-80 kg. During the conduct of the experiment, subjects were asked to stand and sit in the stationary and post-motion state in a real-life setting. We collected data from IR-UWB in three states. In order to test the robustness of the human heartbeat rate extraction method in this paper for IR-UWB devices at different angles as well as at different positions, we set up our experiments at different distances and orientations located relative to the IR-UWB. Figure 6 shows our experimental scenario. We collected a total of 24 hours of IR-UWB data (equivalent to about 120,000 heartbeat cycles) with the corresponding real data collected by the specialized equipment. We divided the data into 30-second segments, yielding a total of 2,880 data samples. We use 30 percent of the samples to train the one-dimensional TCN model, and then for the remaining samples as a test set.

The human heartbeat rate is proposed as an evaluation metric. By using the peak-finding algorithm, we can get the peaks of the corresponding heartbeats in a sample, and extract the time units t corresponding to different peaks. By calculating the time difference between two neighboring peaks, we can get the length of a heartbeat cycle, and then get the bpm value of the heartbeat rate of the human body, which is calculated in the following way:

$$P = \frac{60 \times (N-1)}{\Sigma_{n=1}^{N-1} t_{n+1} - t_n}. \tag{8}$$

B. Overall performance

We carried out a total of 10 groups of experiments in the normal state, each group collected 10 minutes of heartbeat data, every 1 minute to calculate a bpm value. We got the CDF values of the human body in the normal state, which is shown in Figure 7. For the 10 groups of test data, the overall average error is 4.1 bpm, and the recognition accuracy of more than 90 percent of the data is less than 6.7 bpm or less. Considering that the human heart rate is normally 60 bpm-180 bpm, this rate is acceptable, thus demonstrating that the proposed method in this paper meets the efficiency of high-precision heartbeat detection.

C. Impact of different factors

In the following, we investigate the effects of different practical factors. In order to test the robustness of our system for testing the human heartbeat rate, we carried out the relevant tests in a variety of different experimental environments, which are analyzed by four dimensions, namely, different subjects, different distances relative to the IR-UWB device, different angles, and whether or not the subjects are exercising. Next, the specific experimental results will be presented in the form of box-and-line plots, where the upper and lower boundaries of the box are the upper and lower quartiles, the upper and lower horizontal lines are the corresponding maximum and minimum values, the middle horizontal line is the median value and the red points are the average of the whole result.

1) Different subjects: The performance of all seven subjects is shown in Figure 8. As can be seen from the figure, the average error of the human heartbeat rate for the seven subjects was 2.643 bpm per minute, and the highest heartbeat rate error was 6.5 bpm. This result confirms that the performance of the one-dimensional TCN model is actually insensitive to the differences between human subjects and is valid for all subjects.

2) Different distances: Since for IR-UWB devices, as the distance of the pulse signal propagation increases, the signal exhibits a nonlinear attenuation, leading to a decrease in the sensing accuracy, so to evaluate the effect of distance, we set the subject distances to 1.2 m, 2.4 m, and 3.6 m, and collected measurements accordingly, and the results for the accuracy of the human heartbeat rate are shown in Figure 9. The result clearly shows that the distance has a negative effect on the performance, as the distance increases, the reflected signal becomes weaker, the closer the distance corresponds to the higher accuracy of the human heartbeat rate obtained, at a distance of 1.2 m, the average error is 1.5 bpm; at a distance of 2.4 m, the average error is 2.5 bpm; when the distance is increased to 3.6 m, the average error is 9 bpm. For the method proposed in this paper, when the sensing distance is kept between 1.2 m and 3.6 m, it can realize the acquisition of

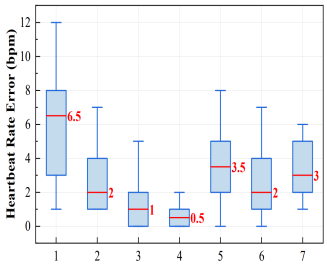

Fig. 8. Impact of different subjects.

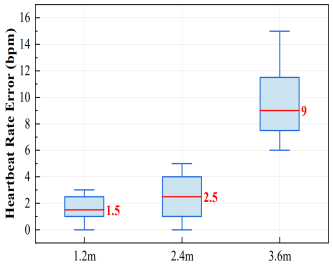

Fig. 9. Impact of different distances.

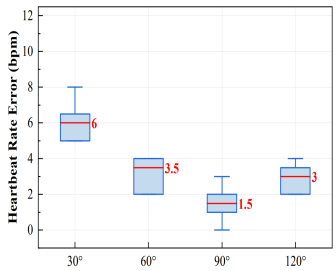

Fig. 10. Impact of different angles.

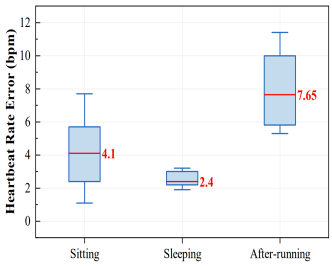

Fig. 11. Impact of different states.

human heartbeat and heartbeat rate with high accuracy, which is enough to meet the needs of daily use.

3) Different angles: Current IR-UWB-based sensing often strictly controls the angle between the terminal and the target. In real scenarios, it's challenging to keep the RF antenna facing the center of the human body due to room layouts. We tested the perception performance at angles of 30°, 60°, 90°, and 120°, with 90° representing the antenna directly facing the target. As shown in Figure 10, the best accuracy (1.5 bpm error) occurs at 90°, while accuracy decreases as the angle increases, with the highest error reaching 6 bpm. Beam constraints likely cause a significant drop in sensing accuracy at wider angles, but fine sensing is possible within a reasonable beam range.

4) Different states: In practice, users' heartbeat rates change due to varying states, so detecting accurate heartbeat rates under different conditions is crucial. We tested subjects in standing, sitting, and post-motion states, as shown in Figure 11. The smallest error (2.4 bpm) occurred in the sleeping state, while the sitting state had an average error of 4.1 bpm, and the post-motion state showed the highest error at 7.65 bpm. These results confirm that our method can accurately estimate the human heartbeat rate in various states by leveraging the periodicity of the heartbeat cycle to generate the autocorrelation matrix.

IV. Conclusion

This paper proposes a heartbeat rate estimation system UWHeart based on the characteristics of the periodic change. The system uses IR-UWB technology to capture the reflection signal of the monitoring target, thus realizing the accurate estimation of the heartbeat rate. We implemented the UWHeart system on a commercial IR-UWB device and monitored the heartbeat rate of 7 subjects for up to 24 hours. The experimental results show that the UWHeart system has an average heartbeat error of 4.1 bpm and maintains highly accurate heartbeat estimation at different distances and angles. This result proves the superiority and practicality of the UWHeart system in the field of contact-free heartbeat monitoring.

References

[1] C. W. Tsao, A. W. Aday, Z. I. Almarzooq, A. Alonso, A. Z. Beaton, M. S. Bittencourt, A. K. Boehme, A. E. Buxton, A. P. Carson, Y. Commodore-Mensah, *et al.*, "Heart disease and stroke statistics—2022 update: a report from the american heart association," *Circulation*, vol. 145, no. 8, pp. e153–e639, 2022.

[2] X. Wang, M. Qi, C. Dong, H. Zhang, Y. Yang, and H. Zhao, "Accurately identifying coronary atherosclerotic heart disease through merged beats of electrocardiogram," in *2022 IEEE International Conference on Bioinformatics and Biomedicine (BIBM)*, pp. 1249–1254, IEEE, 2022.

[3] G. Paterniani, D. Sgreccia, A. Davoli, G. Guerzoni, P. Di Viesti, A. C. Valenti, M. Vitolo, G. M. Vitetta, and G. Boriani, "Radar-based monitoring of vital signs: A tutorial overview," *Proceedings of the IEEE*, 2023.

[4] K. Jiang, S. Liang, L. Meng, Y. Zhang, P. Wang, and W. Wang, "A two-level attention-based sequence-to-sequence model for accurate inter-patient arrhythmia detection," in *2020 IEEE International Conference on Bioinformatics and Biomedicine (BIBM)*, pp. 1029–1033, IEEE, 2020.

[5] A. El Ali, R. Ney, Z. M. van Barlow, and P. Cesar, "Is that my heartbeat? measuring and understanding modality-dependent cardiac interoception in virtual reality," *IEEE Transactions on Visualization and Computer Graphics*, 2023.

[6] J. L. Sarkar, V. Ramasamy, A. Majumder, B. Pati, C. R. Panigrahi, W. Wang, N. M. F. Qureshi, C. Su, and K. Dev, "I-health: Sdn-based fog architecture for iiot applications in healthcare," *IEEE/ACM Transactions on Computational Biology and Bioinformatics*, 2022.

[7] Z. Chen, T. Zheng, C. Cai, Y. Gao, P. Hu, and J. Luo, "Wider is better? contact-free vibration sensing via different cots-rf technologies," in *IEEE INFOCOM 2023-IEEE Conference on Computer Communications*, pp. 1–10, IEEE, 2023.

[8] J. Chen, D. Zhang, Z. Wu, F. Zhou, Q. Sun, and Y. Chen, "Contactless electrocardiogram monitoring with millimeter wave radar," *IEEE Transactions on Mobile Computing*, 2022.

[9] C. Jiao, C. Chen, S. Gou, D. Hai, B.-Y. Su, M. Skubic, L. Jiao, A. Zare, and K. Ho, "Non-invasive heart rate estimation from ballistocardiograms using bidirectional lstm regression," *IEEE Journal of Biomedical and Health Informatics*, vol. 25, no. 9, pp. 3396–3407, 2021.

[10] T. Li, H. Shou, Y. Deng, Y. Zhou, C. Shi, and P. Chen, "A novel heart rate estimation method exploiting heartbeat second harmonic reconstruction via millimeter wave radar," in *ICASSP 2023-2023 IEEE International Conference on Acoustics, Speech and Signal Processing (ICASSP)*, pp. 1–5, IEEE, 2023.

[11] Z. Chen, T. Zheng, C. Cai, and J. Luo, "Movi-fi: Motion-robust vital signs waveform recovery via deep interpreted rf sensing," in *Proceedings of the 27th annual international conference on mobile computing and networking*, pp. 392–405, 2021.

[12] T. Zheng, Z. Chen, S. Zhang, C. Cai, and J. Luo, "More-fi: Motion-robust and fine-grained respiration monitoring via deep-learning uwb radar," in *Proceedings of the 19th ACM conference on embedded networked sensor systems*, pp. 111–124, 2021.

[13] S. Zhang, T. Zheng, Z. Chen, and J. Luo, "Can we obtain fine-grained heartbeat waveform via contact-free rf-sensing?," in *IEEE INFOCOM 2022-IEEE conference on computer communications*, pp. 1759–1768, IEEE, 2022.

[14] Z. Wang, B. Jin, S. Li, F. Zhang, and W. Zhang, "Ecg-grained cardiac monitoring using uwb signals," *Proceedings of the ACM on Interactive, Mobile, Wearable and Ubiquitous Technologies*, vol. 6, no. 4, pp. 1–25, 2023.

[15] H. Zhang, P. Jian, Y. Yao, C. Liu, P. Wang, X. Chen, L. Du, C. Zhuang, and Z. Fang, "Radar-beat: Contactless beat-by-beat heart rate monitoring for life scenes," *Biomedical Signal Processing and Control*, vol. 86, p. 105360, 2023.

[16] Y. Mai, Z. Chen, B. Yu, Y. Li, Z. Pang, and Z. Han, "Non-contact heartbeat detection based on ballistocardiogram using unet and bidirectional long short-term memory," *IEEE Journal of Biomedical and Health Informatics*, vol. 26, no. 8, pp. 3720–3730, 2022.